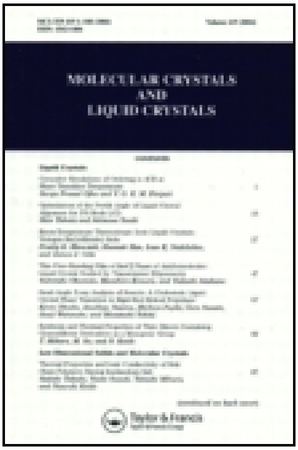

Molecular Crystals and Liquid Crystals Science and Technology. Section A. Molecular Crystals and Liquid Crystals

Publication details, including instructions for authors and subscription information:
http://www.tandfonline.com/loi/gmcl19

Electrochemical Doping of Single Wall Carbon Nanotubes with Lithium

Agnes Claye [a] & John E. Fischer [a]

[a] Department of Materials Science and Engineering and Laboratory for Research on the Structure of Matter, University of Pennsylvania, Philadelphia, PA, 19104, USA

Version of record first published: 24 Sep 2006

To cite this article: Agnes Claye & John E. Fischer (2000): Electrochemical Doping of Single Wall Carbon Nanotubes with Lithium, Molecular Crystals and Liquid Crystals Science and Technology. Section A. Molecular Crystals and Liquid Crystals, 340:1, 743-748

To link to this article: http://dx.doi.org/10.1080/10587250008025557

Mol. Cryst. and Liq. Cryst., 2000, Vol. 340, pp. 743-748
Reprints available directly from the publisher
Photocopying permitted by license only

Electrochemical Doping of Single Wall Carbon Nanotubes with Lithium

AGNES CLAYE and JOHN E. FISCHER

Department of Materials Science and Engineering and Laboratory for Research on the Structure of Matter, University of Pennsylvania, Philadelphia, PA 19104, USA

(Received June 22, 1999; In final form June 25, 1999)

Reversible insertion of Li into purified single wall carbon nanotubes was achieved electrochemically. Galvanostatic charge-discharge and cyclic voltammetry indicated that there is no well-defined redox potential for Li insertion or removal in the nanotube lattice. The Li reversible capacity was found to be 460 mA.h/g, significantly higher than the theoretical value for graphite. *In-situ* X-ray diffraction revealed an irreversible loss of the 2-D triangular lattice upon doping. *In-situ* resistivity measurements presented a 20-fold decrease in resistance upon doping, reversible upon undoping.

Keywords: nanotubes; lithium; electrochemistry; doping

INTRODUCTION

In recent years, tremendous efforts have been devoted to studying the insertion of Li ions into carbon materials, due to their potential application as anodes in rechargeable Li ion batteries. Although most research has focused on graphite [1] and disordered carbons [2], novel forms of carbons such as nanotubes recently attracted some attention for this application [3,4]. We here report on the properties of single-wall carbon nanotubes (SWNT) upon electrochemical doping with Li. We first present the electrochemical characteristics of SWNT, as investigated by galvanostatic charge-discharge and cyclic voltammetry. We then report on the effect of doping on the structure and electronic conductivity of SWNT, as studied by ***in-situ*** X-ray diffraction and ***in-situ*** resistivity measurements.

ELECTROCHEMICAL PROPERTIES OF SWNT

The electrochemical insertion of Li into SWNT was investigated by galvanostatic charge-discharge and cyclic voltammetry experiments on Li/SWNT half-cells. The working electrode consisted of purified SWNT (from the PLV process) in the form of buckypaper, and the electrolyte was 1M $LiPF_6$ in EC:DMC.

The results are presented in Figure 1. During the first reduction, a very large capacity of 1660 mA.h/g was observed, while a reversible capacity of

460 mA.h/g was obtained from the first oxidation. The latter corresponds to a stoichiometry of $Li_{1.23}C_6$ and is 23% larger than the theoretical value for graphite. We attribute the large irreversible capacity (1200 mA.h/g) to electrolyte reduction and formation of a solid electrolyte interface (SEI), as evidenced by the long plateau at 0.9 V in the first discharge. BET measurements indicated that the surface area of SWNT is on the order of 350 m^2/g, which is much larger than that of graphite and explains the large irreversible capacity. No voltage plateau was observed in the charge-discharge curves, indicating the absence of a staging mechanism *via* well-defined interstitial sites traditionally observed for alkali metal doping in graphite or polyacetylene. The large voltage hysteresis between charge and discharge also distinguishes the electrochemical behavior of SWNT from that of Li-GICs.

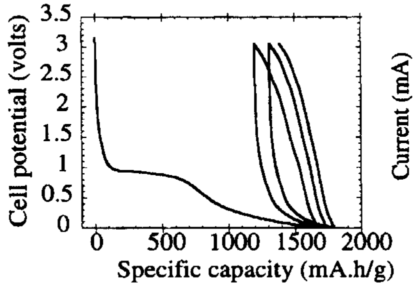

FIGURE 1. Galvanostatic charge-discharge for a Li/SWNT cell (20 mA/g). First 3 cycles are represented.

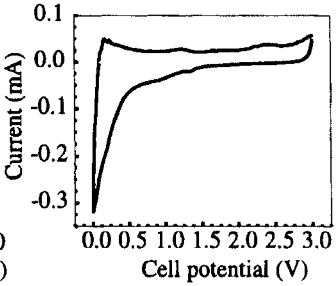

FIGURE 2. Cyclic voltammogram (0.1 mV/s) for a Li/SWNT cell. Third cycle is represented.

The cyclic voltammetry results are presented in Figure 2. The absence of well-defined redox peaks confirms that there is no well-defined potential for Li insertion and removal. Li can be inserted and removed over a wide range of potentials between 0 and 3 volts. These results are consistent with the galvanostatic results and rule out the possibility of staging. The absence of redox peaks in the CV suggests that the Li insertion mechanism is very different from that in graphite, polyacetylene and solid C_{60}, all of which exhibit well-defined reduction and oxidation waves in the cyclic voltammogram [1,5,6].

IN-SITU X-RAY DIFFRACTION OF LITHIUM DOPED SWNT

In-situ X-ray diffraction and electrochemical doping were carried out in an attempt to identify the structural changes imposed by doping in order to understand the Li insertion mechanism in SWNT. SWNT were doped under galvanostatic charge and discharge, interrupted at regular intervals to acquire X-ray spectra. The X-ray data is presented in Figure 3. An X-ray pattern for SWNT before mounting in the electrochemical cell is included in Figure 3(a) for reference. In this spectrum appear the reflections of the SWNT 2-D triangular lattice at 6.3, 10.5, 16.5 and 22 degrees, as well as a sharp peak at 26.4 degrees corresponding to the (002) reflection of graphitic impurities. In all other spectra, the large diffuse peak centered at 22 degrees is due to scattering from the electrolyte. Upon doping, we observed a gradual loss of the SWNT first and second order peaks, which eventually totally disappeared. At very low potentials, we observed a downward shift of the graphite (002) reflection to a value of 25.5 degrees corresponding to the (001) of LiC_6. This shows that the graphitic impurities have been intercalated. Upon undoping, the graphite peak recovered its original position, indicating the deintercalation of the graphitic impurities. No recovery of the SWNT reflections was observed upon undoping, suggesting an irreversible loss of the triangular lattice. Crystallinity could be restored by a 1200°C vacuum anneal. The observed loss of crystallinity, although not well understood, is consistent with the disorder in the rope lattice observed by O. Zhou *et al* when doping SWNT with K and Cs [7].

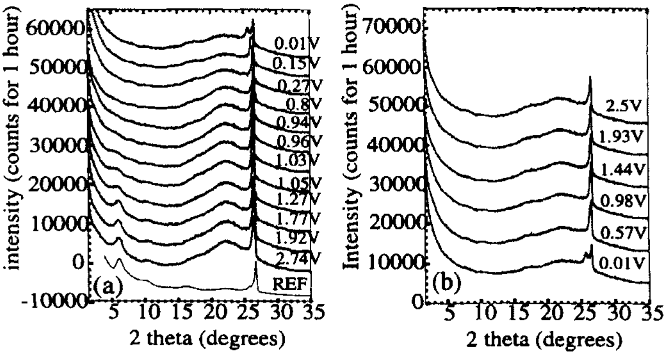

FIGURE 3. *In-situ* X-ray diffraction profiles of SWNT as a function of (a) doping (b) undoping. Included at the bottom of (a) is a reference profile for the dry sample.

IN-SITU RESISTIVITY OF LITHIUM DOPED SWNT

In-situ 4-point resistivity measurements and electrochemical doping were carried out in order to study the changes in electronic conductivity of SWNT upon doping. Figure 4 presents the results for 2 cycles of galvanostatic charge-discharge using 1M $LiPF_6$ in EC:DMC as the electrolyte.

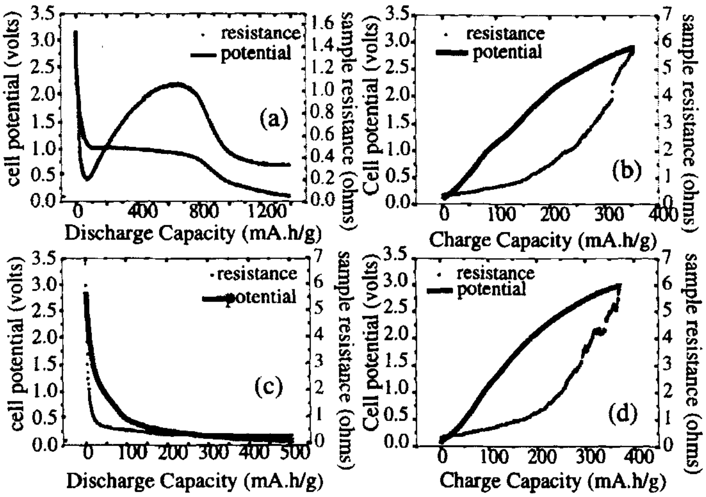

FIGURE 4. In situ 4-point resistivity on Li-doped SWNT in 1M $LiPF_6$ in EC:DMC. Two galvanostatic cycles are represented: (a) 1rst reduction, (b) 1rst oxidation (c) 2nd reduction (d) 2nd oxidation.

During the first reduction (Figure 4a), we observed a 7-fold drop in resistance as the cell potential decreased from 3 volts to 0.9 volts. At 0.9 volts, the SEI started forming, leading to a steady increase in resistance throughout the reduction plateau corresponding to surface passivation. This is due to the electrically insulating nature of the SEI, worsening the inter-rope and inter-tube contacts. After completion of the SEI, the resistance decreased steadily upon further doping. Upon undoping (Figure 4b), the resistance increased continuously as we removed Li. The resistance of the pristine sample was not fully recovered because of the presence of the SEI. During further cycling (Figure 4c and d), no SEI effect was observed, such that the resistance reversibly decreased and increased upon doping and undoping, respectively. The observed change in resistance between the fully doped and dedoped state is a factor of 20. Interestingly, most of the resistance drop upon doping took place at fairly dilute doping levels ($Li_{0.1}C_6$). A hysteresis can be observed in the resistance between doping and undoping, similar to the voltage hysteresis in the electrochemical data.

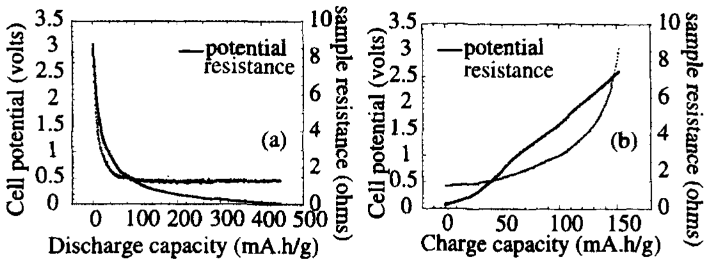

FIGURE 5. In situ 4-point resistivity on Li-doped SWNT in 1M $LiPF_6$ in THF. First cycle of galvanostatic discharge (a) and charge (b) is represented.

In order to avoid the corruption of the data due to SEI formation, we repeated the experiment using an electrolyte which is known not to create an SEI, namely 1M $LiPF_6$ in THF. The results from the first galvanostatic charge-discharge are presented in Figure 5. No SEI formation was observed, such that the resistance reversibly decreased and increased upon insertion and removal of the Li, respectively. Note that in the case of THF, solvent molecules are likely to solvate the Li ions and to co-intercalate in the host structure, as in GICs. This explains the lower Li capacities observed with the THF solvent. Subsequent cycles exhibited very similar results.

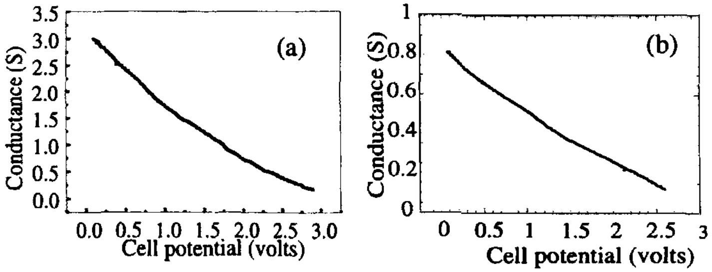

FIGURE 6. *In-situ* conductance of Li-doped SWNT as a function of cell potential in (a) EC:DMC $LiPF_6$ and (b) THF $LiPF_6$. Data shown was obtained upon first oxidation of the cells.

Figure 6 presents the data of Figures 4 and 5 in a different fashion: here we plot conductance vs. cell potential. Interestingly, the conductance varies almost linearly with cell potential in both electrolytes. Since the conductance is proportional to the density of states at the Fermi level, and since the electrochemical potential is related to the Fermi energy of the material, this relationship can give information about the density of states for bulk SWNT material. In that regard, further work remains to be done in order to establish the exact relationship between the electrochemical potential of the cell and the Fermi level of the material.

CONCLUSIONS

Reversible insertion of Li into SWNT was achieved electrochemically. The Li reversible capacity is on the order of 460 mA.h/g, significantly higher than that of graphite. However, the large irreversible capacity and the large voltage hysteresis limit the attractiveness of SWNT for battery applications. The Li insertion mechanism is not well understood. Cyclic voltammetry and galvanometry have ruled out the hypothesis of a staging mechanism. *In-situ* X-ray diffraction showed that doping induces irreversible disorder in the triangular lattice. On the other hand, *in-situ* resistivity measurements showed a reversible decrease in resistance upon doping, suggesting a charge transfer between Li and carbon. Further work remains to be done in order to determine where the Li ions go.

Acknowledgments

Research supported by the NSF MRSEC Grant DMR96-32598. We are grateful to the group of R. Smalley at Rice University for providing the purified SWNT material.

References

[1] M. D. Levi, E. A. Levi, D. Aurbach, *J. Electroanal. Chem.*, **421**, 89 (1997).
[2] J. R. Dahn, T. Zheng, Y. Liu, X. S. Xue, *Science*, **270**, 5236 (1995).
[3] B. Gao, A. Kleinhammes, C. Bower, L. Fleming, Y. Wu, O. Zhou, this volume.
[4] E. Frackowiak, S. Gautier, H. Gaucher, S. Bonnamy, F. Beguin, *Carbon*, **37**, 61 (1999).
[5] T. R. Jow, L. W. Shacklette, *J. Electrochem. Soc*, **135**, 3, 541 (1988).
[6] Y. Chabre, D. Djurado, M. Armand, W. Romanow, N. Coustel, J. P. McCauley, J. E. Fischer, A. B. Smith, *J. Am. Chem. Soc.*, **114** (2), 764 (1992).
[7] S. Suzuki, C. Bower, O. Zhou, *Chem. Phys. Lett.*, **285**, 230 (1998).